Fiber optic Raman sensor to monitor the concentration ratio of nitrogen and oxygen in a cryogenic mixture

Vidhu S. Tiwari,[1] Rajamohan R. Kalluru,[2] Fang Y. Yueh,[1] Jagdish P. Singh,[1,*] William St. Cyr,[3] and Sunil K. Khijwania[4]

[1]Institute for Clean Energy Technology, Mississippi State University 205 Research Boulevard, Starkville, Mississippi 39759, USA
[2]Mississippi Ethanol LLC, 86 Industrial Park Boulevard, Winona, Mississippi 38968, USA
[3]NASA/Stennis Space Center (SSC), Stennis, Mississippi 39529, USA
[4]Department of Physics, Indian Institute of Technology, Guwahati, Assam 781039, India

*Corresponding author: singh@ICET.msstate.edu

A spontaneous Raman scattering optical fiber sensor was developed for a specific need of the National Aeronautics and Space Administration (NASA) for long-term detection and monitoring of the purity of liquid oxygen (LO_2) in the oxidizer feed line during ground testing of rocket engines. The Raman peak intensity ratios for liquid nitrogen (LN_2) and LO_2 with varied weight ratios (LN_2/LO_2) were analyzed for their applicability to impurity sensing. The study of the sensor performance with different excitation light sources has helped to design a miniaturized, cost-effective system for this application. The optimal system response time of this miniaturized sensor for LN_2/LO_2 measurement was found to be in the range of a few seconds. It will need to be further reduced to the millisecond range for real-time, quantitative monitoring of the quality of cryogenic fluids in a harsh envioronment.   © 2007 Optical Society of America

OCIS codes: 0300.6450, 300.6330, 300.0300, 140.3550, 170.5660, 060.2370.

1. Introduction

The escalating use of liquid phase elements like oxygen and hydrogen as cryogenic fuels and the consequent need for monitoring their quality led to the development of a variety of sensor systems. Several types of electronic sensor, such as capacitance-based and electrochemical sensors, are commercially available but lose their reliability in the supercritical environment of rocket engines, where low temperatures and high pressures severely inhibit their optimal performance [1–3]. The high flow rate of the oxidizer feed lines poses a serious limitation on the accurate measurement of impurity levels in cryogenic oxygen and requires a sensor system with a fast response time. Quantitative detection of impurities in oxygen is critical for this technologically important application [4]. Application of fiber optic technology offers an alternative approach to measuring various parameters of interest and addresses several measurement issues associated with characterizing the cryogenic fuels feeding a rocket engine. Today, optical fiber sensing technology has evolved to the point where one can measure nearly all the physical parameters of interest and a very large number of chemical species as well [5]. Schmidt and Sanders [6] reported the differential absorption sensor applied for liquid oxygen (LO_2) measurements. A computational-analytical technique for quality maintenance in cryogenic liquid methane at the entrance to the test article tank has been reported [7].

The present work is motivated by a specific need of the National Aeronautics and Space Administration (NASA) for detection and monitoring of the quality of LO_2 in the delivery line during ground testing of rocket engines. Online, near-real-time characterization of cryogenic fluid mixtures like liquid nitrogen (LN_2) and LO_2 by optical diagnostics is an area that has not yet been explored to the best of our knowledge. We report the first phase of the development of an all-optical cryogenic fluid sensor based on Raman

spectroscopy, in conjunction with fiber optics. The sensor under study can be used to infer the abundance of impurities in a rocket engine fuel feed line. An attractive design feature of a fiber optic sensor lies in the capability for real-time, *in situ* qualitative as well as quantitative determination of LO_2 and/or LN_2 from their mixtures through the Raman spectral analysis. Various issues involved in monitoring supercritical fluid mixtures, such as sample vaporization and condensation, system optimization, signal-to-noise ratio, and other safety parameters, have been well addressed and provide a novel vision for encountering challenges involved in process and control of cryogenic fuels.

Optical fiber sensors have certain distinct advantages over conventional sensors, such as remote sensing, multiplexing and distributed sensing, and immunity toward electromagnetic signals, that make them more advantageous in practical applications. Laser Raman spectroscopy has been known for years as a relatively simple analytical method for identification of molecules in gases, liquids, and solids. Raman spectroscopy is based on the Raman effect that results from energy exchange between incident photons and the scattered molecules [8]. The Raman scattered light occurs at frequencies that are shifted from the incident laser light by the change in vibrational, rotational, or electronic energies of a molecule. By measuring the frequency and intensity of light inelastically scattered from the sample, the molecules in the sample can be qualitatively and quantitatively characterized. To explore various possibilities of employing a low-cost, portable optical sensor based on laser Raman spectroscopy in the harsh environment of a rocket engine, we evaluated three excitation light sources for the sensor. Two frequency-doubled 532 nm cw Nd:YAG lasers (TEM_{00} and multimode) were first used as the excitation light source with a fiber optic miniaturized Raman probe. Then a diode laser operating at 670 nm was used as the excitation source in an attempt toward configuring a cost-effective optical sensor that fulfills the needs of various national laboratories and cryogenic industries.

2. Experimental Details

The main focus of this research effort was to develop a real-time optical fiber sensor that employs a cw 532 nm laser as an excitation light source for monitoring the concentration of LN_2 in LN_2 and LO_2 mixtures. In the process of developing a miniaturized and cost-effective optical fiber Raman sensor, we also evaluated a diode laser as an excitation light source. The details of the excitation sources used in this study are given in Table 1.

In the initial experiment, an optical fiber Raman sensor is set up using a frequency-doubled 532 nm cw Nd:YAG laser (Coherent DPSS 532) as the excitation light source, with maximum output power of 330 mW. The laser output energy was attenuated through the use of neutral-density filters to protect the fiber in the excitation arm of the probe from potential damage by high-intensity light. A block diagram of the experimental setup is shown in Fig. 1(a). This sensor configuration employed a modified In-Photonics fiber optic miniaturized Raman probe. The probe consisted of just two parallel optical fibers; one (90 μm core diameter) guided the incident light to a liquid sample mixture enclosed within a Dewar, whereas the other (200 μm core diameter) collected the emitted Raman signal and fed it to an Ocean Optics spectrometer (USB 2000). This spectrometer had a 1200 line/mm grating along with a 2048-element CCD detector attached to the exit of the spectrograph and was interfaced with a computer via a USB port. The spectral range of the spectrometer is from 550 to 858 nm. Probe performance in terms of Raman signal response and background noise level was improved by incorporating a miniaturized lens at the tip of the probe with a working distance of about 30 mm. The sample mixture was prepared with different concentration ratios of LN_2 and LO_2. The Raman spectrum of each set of sample mixture was recorded with an integration time (IT) of 300 ms and averaged (Avg) over 10 spectra, resulting in a 3 s (IT × Avg) data acquisition and recording time. The data acquisition parameters (integration time and average) were chosen so as to have a minimum time for recording mixture data while taking into consideration that the phase of the sampling mixture was rapidly changing from liquid to gas. Owing to the low temperature of the liquid mixture, the greatest challenges of the experiment were minimization of vaporization loss and also determination of the accuracy with which the weight ratio of the sample constituents was determined during preparation of the mixtures. In the initial experiment, a cap with a hole was mounted on the Dewar. Though it allowed a clear passage from the probe for the laser light to focus onto the LN_2/LO_2 mixture, it could not prevent the

Table 1. Details of the Excitation Sources

Excitation Source	Wavelength (nm)	Laser Linewidth (nm)	Max. Power (mW)	Beam Diameter[a] (mm)	Transverse Mode
532 nm laser					
Coherent	532	0.00047	330	0.70	TEM_{00}
Milles Griot	532	0.18	3000	0.24	Multimode
670 nm diode laser	670	0.70	700	1.5	Multimode
Power Technology Inc.					

[a]$1/e^2$ at waist.
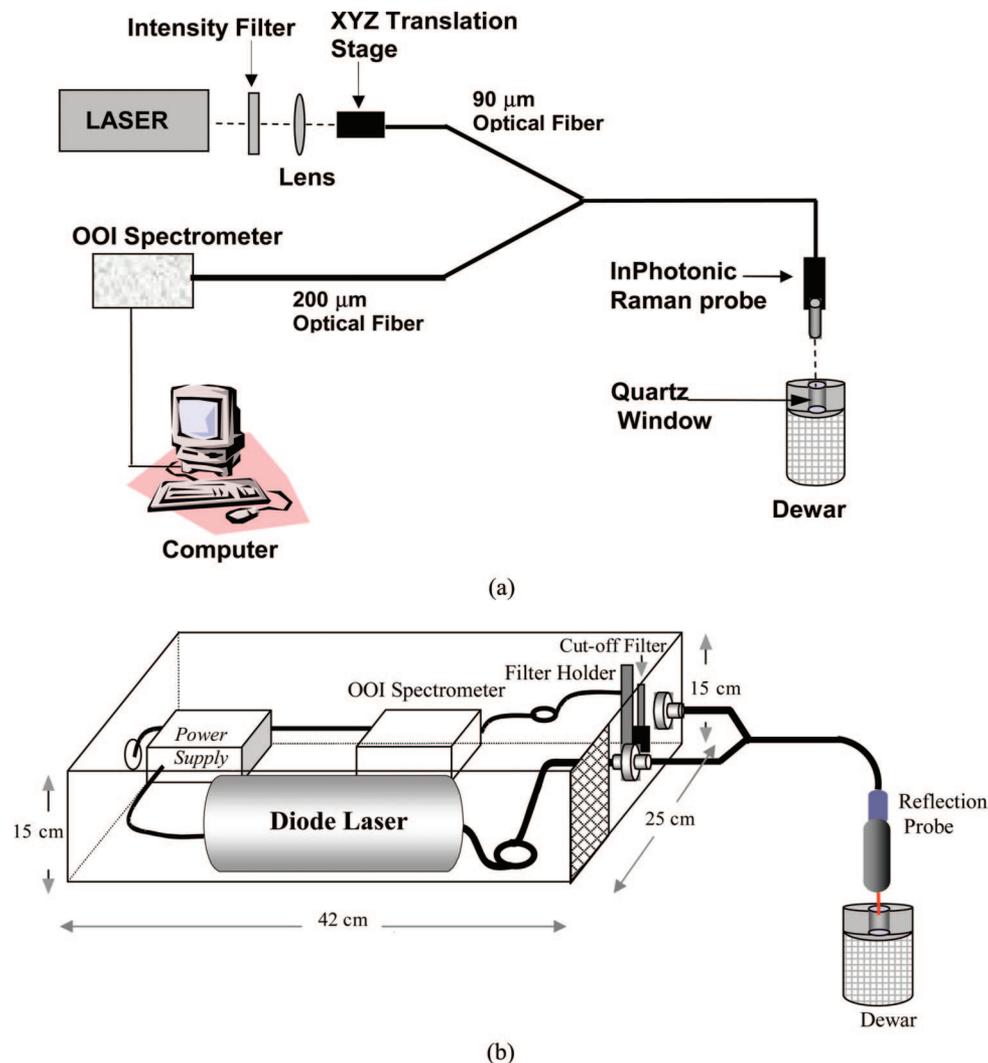
Fig. 1. (Color online) Experimental setup of the optical fiber Raman sensor: (a) system based on an InPhotonic Raman probe and (b) prototype Raman system based on a reflection probe.

vapors from escaping and condensing onto the tip of the fiber probe. Condensation of vapors onto the tip of the probe, over a prolonged time, would have affected the coating of the lens at the tip of the probe. Therefore, to overcome this problem, two identical quartz windows [0.25 in. (0.64 cm)] were introduced into the Dewar cap hole, which prevented vapors from reaching the tip of the probe. Attenuation of the laser light was observed to result from the introduction of the quartz windows and increased as the vapors from the sample mixture condensed on the surface of the quartz windows, resulting in an overall reduction of signal-to-noise ratio of the Raman signal. Laser power was further increased to compensate for the attenuation in the laser light falling onto the sample mixture. Also, a heat gun was installed in the vicinity of the Dewar cap to minimize condensation of vapor on the surface of the quartz window facing the sample mixture. As a result, long-term stable operation of the Raman sensor could be achieved.

To study the effect of laser properties on the Raman signal, the Raman spectra produced by a narrowband

532 nm laser (Coherent DPSS 532) and by a high-power, inexpensive, broadband 532 nm laser (Milles Griot GHS 309) were compared. The experimental configuration was kept the same for both lasers, except a neutral-density filter was employed with the broadband 532 nm laser output to attenuate the laser power so that the laser power on the sample mixture was ~140 mW from either laser.

A prototype Raman sensor based on a 700 mW, cw diode laser (Power Technology), operating at 670 nm, as an excitation light source and a Y-shaped reflection–backscattering probe (Ocean Optics, R200-REF) was designed and evaluated. Figure 1(b) is a schematic diagram of this system. This Y-shaped probe consists of seven optical fibers, each having a 200 µm core diameter and a 0.22 numerical aperture with one launching fiber and six surrounding collection fibers. The uniqueness of the prototype sensor lies in its compact design configuration that includes carefully aligned optical components, namely, laser diode, filter holder, long-wave pass–cutoff filter (725 nm) and a compact spectrometer (Ocean Optics, USB

2000). The compact spectrometer is similar to the one in Fig. 1(a), but the spectral range is from 695 to 965 nm. Raman spectra of mixtures of LO_2 and LN_2 of different concentration (weight) ratios were recorded with prototype Raman sensor in the same manner as described above.

3. Results and Discussions

The present study was primarily focused on quantitative as well as qualitative analysis of LO_2 and LN_2 mixtures at varied levels of their weight ratio. The mixture sample was prepared by adding LO_2 to LN_2 because the molecular weight of oxygen is higher than nitrogen, therefore suppressing the rate of vaporization of LN_2 [9]. The Raman spectrum recorded for a 40% LO_2 and 60% LN_2 (LN_2/LO_2 ~1.5) mixture is shown in Fig. 2(a). Raman bands for LO_2 (~580 nm) and LN_2 (~607 nm), corresponding a Raman shift for O_2 of 1556.4 cm^{-1} and for N_2 of 2330.7 cm^{-1}, are indicated on the spectrum [10]. The concentration ratio of LN_2 and LO_2 was varied from 0.01 to 1.00 at normal atmospheric pressure and temperature while total mixture weight of 100 g was maintained. The Raman band intensity corresponding to LN_2 increased as the relative concentration of LN_2 in the sample mixture increased against the LO_2 as shown in Fig. 2(b). A narrowband Coherent cw Nd:YAG laser, operating at 532 nm, was used in this experiment.

The observed Raman bands of LO_2 and LN_2 were analyzed in terms of spectral band shape, signal-to-noise ratio, and peak intensity. The peak intensity ratio corresponding to Raman bands of LN_2 and LO_2 at various concentrations of their weight ratio was estimated for the calibration curve shown in Fig. 3. Sensor response exhibited a linear trend within the LN_2 and LO_2 concentration ratio limit of 0 to 1.5 and was observed to saturate for the concentration ratio

(a)

(b)
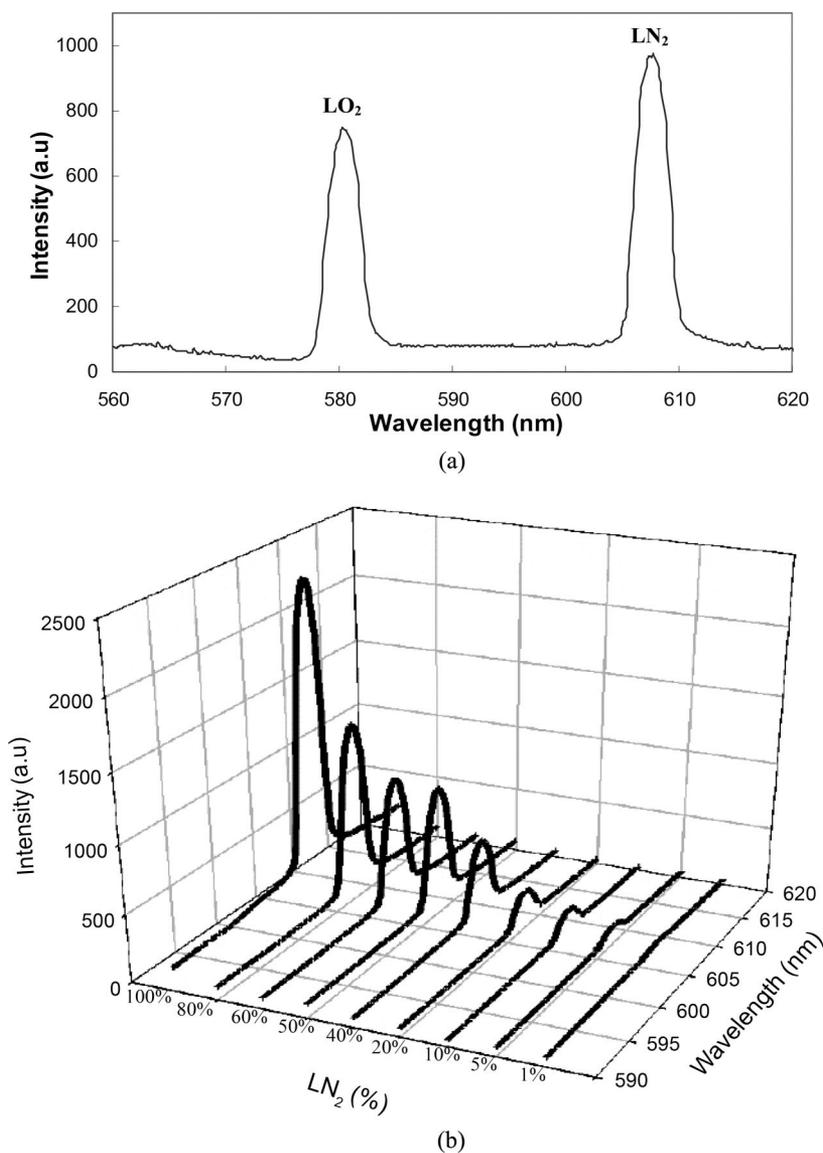
Fig. 2. (a) Raman spectrum of a 40% LO_2 and 60% LN_2 (LN_2/LO_2 ~1.5) mixture. Laser wavelength, 532 nm. (b) Sensor response to the LN_2 and LO_2 mixture as a function of LN_2 concentration.
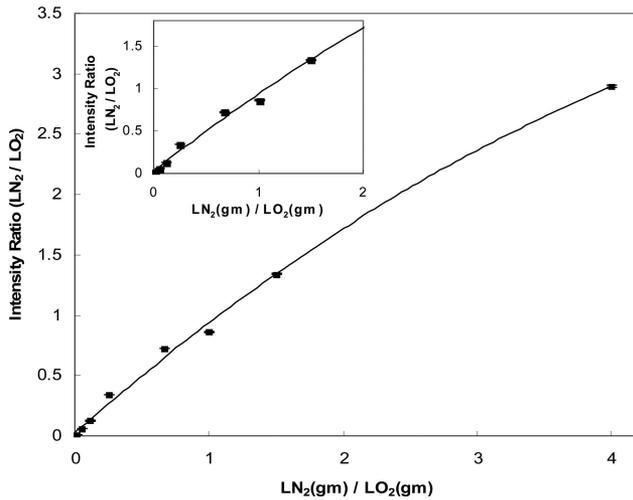
Fig. 3. Intensity ratio variation of LN_2 and LO_2 against their weight ratios.

range (LN_2/LO_2) of 1.5 to 4. The lower signal response of the sensor at higher concentration ratios of LN_2/LO_2 was attributed to the fact that the vaporization rate of LN_2 increased, resulting in the formation of a cloud of a semiliquid gaseous phase mixture and thereby affecting the sensor performance. The spectral band area ratios of Raman LN_2 and LO_2 peaks were also calculated. This calculation was performed for all the sets of spectra corresponding to a particular concentration ratio of LN_2 and LO_2 and was averaged to obtain a single data point. As a result, error due to fluctuations of peak intensity was minimized. Finally, a calibration curve was drawn between the averaged spectral band area ratios of Raman LN_2 and LO_2 peaks as a function of the corresponding weight ratios, as shown in Fig. 4. The following conclusions have been drawn from the above experimental results.

First, the sensor system is capable of successfully monitoring the LN_2 concentration in a LN_2 and LO_2 mixture. Second, the Raman peak area follows the
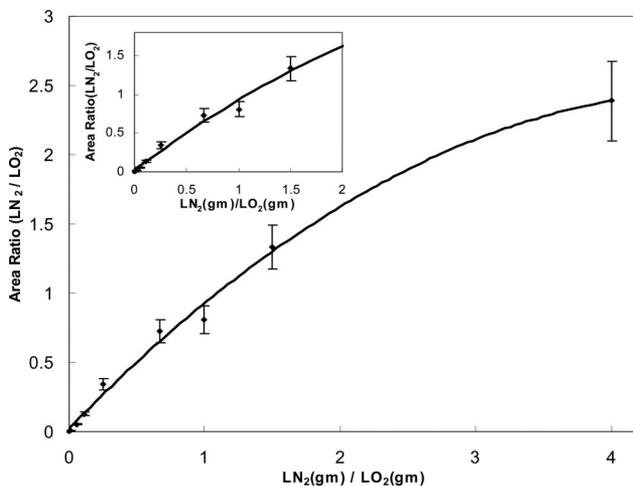
Fig. 4. Area ratio variation of LN_2 and LO_2 against their weight ratios.

same characteristics as the intensity ratio curve. For example, both intensity ratio and area ratio curves exhibit a linear trend within a range of low concentration ratios of LN_2 and LO_2 (LN_2/LO_2 below 1.5) but tend to saturate for LN_2/LO_2 ratios more than $\sim$1.5. This implies that the sensor has high detection sensitivity in the low concentration ratio range and can measure a LN_2 percentage as low as 1% in a sample mixture. For a typical sample mixture of 60% LN_2 and 40% LO_2 (LN_2/LO_2 $\sim$1.5), the limit of detection (LOD) of the sensor was calculated to be $\sim$1%. Also, intensity/area ratio data points fluctuate less as reflected by the error bars on the calibration curves, which are barely visible in Fig. 3. This signifies not only the long-term stable operation of the sensor, but also the reproducibility in the sensor response toward analyte concentration. Although the calibration curve obtained by area ratio method involved statistical averaging of multiple sets of spectra, it did not provide better sensor response. The linear calibration data for the LN_2/LO_2 ratio indicate that the fiber optic Raman sensor has a great potential for qualitative as well as quantitative monitoring of sample constituents in supercritical LN_2 and LO_2 mixtures.

To develop a less expensive sensor for this application, the feasibility of using an inexpensive, high-power, broadband laser (Melles Griot) operating at 532 nm as an excitation light source was tested. Using the same laser energy as with the Coherent laser ($\sim$140 mW) and the same experimental setup, spectra were recorded for various concentration ratios of LO_2 and LN_2 and compared with those obtained by using the 532 nm Coherent laser. Since the spectrometers used in this work have low optical resolution ($\sim$3 nm), the laser beam quality did not play an important role in the observed spectral feature. Comparative analysis of spectra recorded with the two lasers suggests that in both cases spectra share common features and, depending on requirements, either of these could be employed as the excitation light source. The laser linewidth of the Melles Griot laser ($\sim$0.18 nm) is wider than that of the Coherent laser ($\sim$0.00047 nm) and showed slightly higher spectral background in comparison with the Coherent laser. Also, the Melles Griot laser could be operated in the high range of power that is suitable for trace $LN_2/$ LO_2 monitoring.

To develop a prototype sensor using a 670 nm diode laser from Power Technology, the performance of the sensor was first estimated by considering the laser energy and detector response near 532 and near 670 nm. Since the Raman cross section depends inversely on the fourth power of the laser wavelength (λ) [10], the Raman signal is also affected by the excitation wavelength. The various parameters that can affect the Raman signal are summarized in Table 2. Estimation based on these parameters (the effects of optical response from other optics at these two wavelengths were not included in this calculation) shows that the prototype sensor should provide an approximately 4.4 times lower signal than with the system with the more expensive 532 nm excitation

Table 2. Estimation of the Raman Signal from 532 and 670 nm Lasers

	532 nm Laser	670 nm Diode Laser
Maximum laser power on sample	140 mW	380 mW
CCD detector efficiency	2.3	0.4
Grating efficiency	60%	72%
Relative Raman cross section (λ^{-4})	12.48	4.96
Overall relative Raman signal	4.44	1

source. This signal level should be good enough for this type of application.

A typical spectrum of 60% LN_2 and 40% LO_2 (LN_2/LO_2 ~1.5) in the sample mixture, recorded with the prototype sensor by using the 670 nm laser as the excitation light source, is shown in Fig. 5(a), where the LN_2 Raman peak corresponds to ~795 nm and the LO_2 peak corresponds to ~749 nm, respectively. The LOD of LN_2 was estimated from the signal-to-noise ratio found from the Raman spectrum of 60% LN_2 and 40% LO_2 (LN_2/LO_2 ~1.5). The LOD of LN_2 with the prototype sensor was found to be ~20%, which is much higher than the LOD of LN_2 of ~1%
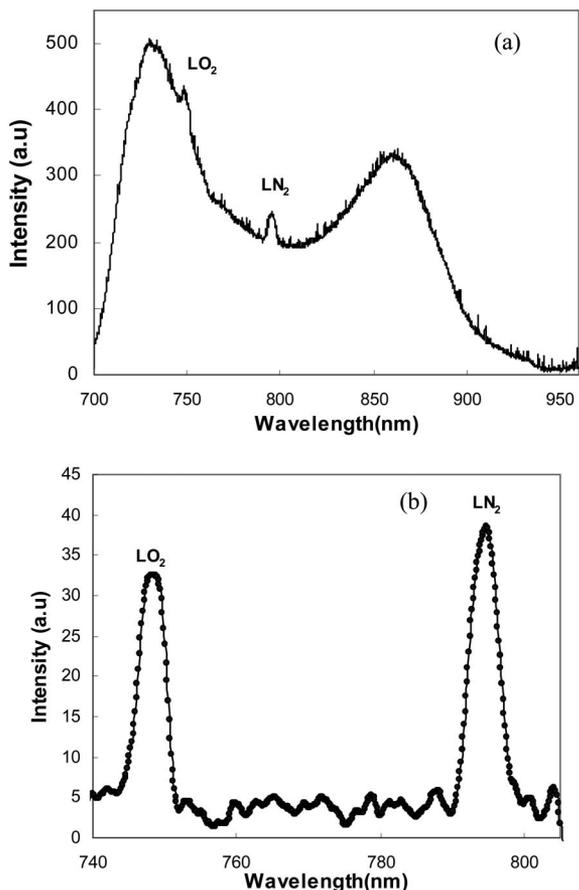
Fig. 5. Raman spectrum for 60% LN_2 and 40% LO_2 (LN_2/LO_2 ~1.5) with the 670 nm diode laser: (a) raw spectrum, (b) background-subtracted spectrum.

found from the sensor by using a 532 nm laser [see Fig. 1(a)]. The spectrum recorded with the 670 nm laser diode also shows a strong background that severely affects the Raman signal of LO_2/LN_2. The overall spectral quality (signal-to-noise ratio) of the prototype sensor with the 670 nm diode laser is not as good as that observed with a 532 nm laser [see Fig. 2(a)]. The performance of the sensor systems with different lasers is actually determined by many factors, such as the spectral characteristics of the laser systems, the optics, and the scattered light. Because of the broadband spectral linewidth of the 670 nm laser diode, a long-wave pass–cutoff filter, centered on 725 nm, is unable to suppress the scattered incident laser light. The scattered light has contributed to part of the strong background observed. The optical fiber can also give rise to a Raman spectral feature and also a fluorescence background signal that is superimposed on the LO_2 and LN_2 spectrum. The current prototype sensor is compact but is unable to effectively remove these background features. To suppress the background and to improve the signal-to-noise ratio of the Raman signal, appropriate combinations of various filters will need to be tested and added to the collection optics of the miniaturized prototype sensor. However, some data processing techniques can be applied to improve the quality of the data. Figure 5(b) shows the processed Raman LO_2 and LN_2 spectrum of the prototype sensor. This spectrum was obtained by subtracting the raw data from the background spectrum (the background spectrum was obtained by fitting with some polynomial functions). Spectral averaging can also be applied to further improve the signal-to-noise ratio. Intensity ratios for LN_2 and LO_2 weight ratios of 1.5 were calculated to be ~1.4 from background-subtracted spectrum obtained from the prototype sensor. The intensity ratios obtained with a 532 nm laser for the same weight ratios of LN_2 and LO_2 is about 1.3.

4. Conclusions

We have presented an optical fiber Raman sensor suitable for cryogenic applications and evaluation of the sensor performance with different excitation light sources. The sensor performance with two different 532 nm lasers and an InPhotonic probe was demonstrated. Efficient light collection optics and good signal-to-noise ratio of the Raman LN_2/LO_2 signal make these laser-based sensor systems an effective tool for rapid as well as sensitive monitoring of LN_2/LO_2 during the testing of a rocket engine. To design a low-cost, reliable sensor for this type of application, we have also tested with a compact, inexpensive diode laser. Although this miniaturized prototype sensor system yielded low signal-to-noise ratio of Raman LN_2/LO_2 signal with appropriate data processing techniques the extracted intensity ratio of the Raman signal of LN_2 and LO_2 is close to that obtained with the more expensive 532 nm excitation systems. This miniaturized diode laser sensor system offers a great deal of flexibility and provides a cost-effective solution for measuring the quality as well as

quantity of cryogenic fluids. However, because of the relatively poor signal-to-noise ratio and background problem, the performance of the current diode laser sensor system is not suitable for real-time monitoring. On the other hand, the system with the high-power 532 nm laser can offer good quality LN_2/LO_2 spectra with a reasonable response time, and therefore it is more suitable for real-time applications. Future research will focus on improving the performance of the sensor for cryogenic liquids under high pressure.

References

1. R. Parry, G. Claborn, A. Haas, R. Landis, W. Pages, and J. Smith, "A high reliability oxygen deficiency monitoring system," presented at the Particle Accelerator Conference, Washington D.C., 17–20 May 1993.
2. M. A Nurge, R. Youngquist, and D. Walters, "Capacitance based mass metering for cryogenic fluids," Cryogenics **43,** 501–506 (2003).
3. J. A. Akintunde, "Simple liquid nitrogen level monitor using copper wire as a sensor," Cryogenics **27,** 266–268 (1987).
4. R. N. Ghosh, G. L. Baker, C. Ruud, and Daniel G. Nocera, "Fiber-optic oxygen sensor using molybdenum chloride cluster luminescence," Appl. Phys. Lett. **75,** 2885–2887 (1999).
5. K. T. V Grattan and B. T. Meggitt, *Optical Fiber Sensor Technology* (Kluwer Academic, 1999).
6. J. R. Schmidt and S. T. Sanders, "Differential absorption sensor applied for liquid oxygen measurements," Appl. Opt. **44,** 6058–6066 (2005).
7. A. M. Domashenko and Y. A. Kondrashkov, "Technology of quality control of liquefied methane-A fuel for space rocket systems," Chem. Pet. Eng. **39,** 656–661 (2003).
8. M. J. Pelletier, *Analytical Applications of Raman Spectroscopy* (Blackwell Science, 1999).
9. P. Atkins and J. de Paula, *Physical Chemistry* (W. H. Freeman, 2003).
10. G. Herzberg, *Spectra of Diatomic Molecules* (Van Nostrand Reinhold, 1950).